Spacecraft Collision Avoidance Using Coulomb Forces with Separation Distance and Rate Feedback

Shuquan Wang* and Hanspeter Schaub†
University of Colorado at Boulder,
Boulder, Colorado 80309

A two-spacecraft collision avoidance problem is discussed in this paper. The spacecraft are assumed to be floating freely in deep space. A control strategy using cluster internal coulomb forces is developed to prevent a collision of the two spacecraft. The control law is designed to keep the separation distance greater than a specified constraint value, and is also designed to keep the departure relative kinetic energy at the same level with the approach kinetic energy. Further, this strategy requires only the measurements of the separation distances and the distance rates. If the achievable spacecraft charge levels are limited, then it is not guaranteed that the collision can always be prevented. Formulating the relative motion of the charged spacecraft using the concepts of orbital mechanics allows us to analyze the conditions under which a collision can be avoided. Given an initial separation distance and distance rate, the minimum spacecraft charge limit required to guarantee collision avoidance is determined. Or, inversely, when the limitations of charges are given, the maximum approach speed at which a potential collision can be avoided is estimated. Numerical simulations illustrate the analytical results.

I. Introduction

COLLISION avoidance is a general concern in a tightly flying cluster of spacecraft with separation distances ranging from dozens to hundreds of meters. Such mission concepts include small satellite swarms flying scenarios where a smaller spacecraft is circumnavigating and inspecting a secondary craft. The concept of a spacecraft formation involves multiple satellites that work together in a group to accomplish the objective of a larger, usually more expensive, satellite. The spacecraft swarm concept envisions a large number of satellites flying in space with loose position-keeping requirements, while the swarm members provide a highly distributed and redundant sensor platform. Collisions can occur when spacecraft within the cluster have control or sensor failures, or lack a guidance strategy to guarantee collision avoidance among a large number of cluster members. Preventing collisions has many challenges. First, the collision onset must be sensed with sufficient accuracy to warrant a corrective maneuver. Second, a control strategy must be developed to provide the required small corrective forces without causing plume-impingement issues on neighboring satellites. This paper focuses on a mission scenario in which loosely clustered satellites are flying in deep space in a bounded configuration. The satellites are assumed to have a low approach speed with respect to each other. This strategy is not designed to repel high-velocity bodies.

Many studies have been published on spacecraft collision avoidance. Slater et al. [1] discuss the collision probability of a formation under the influence of orbital disturbances, and presents requirements for velocity corrections to avoid collision. Singh and Hadaegh [2] consider a minimum effort collision avoidance strategy for a two-spacecraft formation. Campbell and Udrea [3] provide a methodology to monitor the collision probability for satellite clusters. The aforementioned publications mainly concern the collision probability of a formation or a satellite cluster in a long-term orbit mission. Daniel P. Scharf in Reference [4] develops a reactive collision avoidance algorithm for multiple spacecraft collaborating in two-dimensional space. An acceleration-limited, fuel-optimal, collision avoidance trajectory is calculated using a model predictive control while addressing the uncertainties in the motion of colliding spacecraft. This algorithm is a short-term instant trajectory control with the time scale of the algorithm on the order of minutes.

So far, most studies on spacecraft collision avoidance have been based on the control strategies' capability to control all three components of the thrust vector in three-dimensional space. In addition, these control strategies use propellant, which will increase the fuel budget. Fuel-efficient relative motion control is a critical factor for long-term spacecraft cluster or swarm missions because relative orbit correction burns will have to be performed far more often than with conventional formation flying concepts. Further, employing conventional thrusters when spacecraft are flying less than 100 m apart is very challenging because the associated hot and corrosive plume may damage the devices on the neighboring spacecraft.

To perform efficient collision avoidance maneuvers in a dense spacecraft cluster, this paper presents a new approach that uses only electrostatic (coulomb) forces. For tight clusters with spacecraft less than 100 m apart, this approach stands out because the coulomb-force generation is essentially propellantless. Further, it will not generate any propellant plume-impingement issues which could threaten neighboring spacecraft. The use of coulomb thrusting in spacecraft cluster flying has been studied frequently since King et al. originally discussed coulomb formation flying (CFF) in [5].

The concept of CFF uses coulomb forces to achieve the desired relative motion. Spacecraft will naturally charge to nonzero potentials in a space plasma environment. With CFF, the spacecraft charge level is actively controlled through the continuous emission of electrons or ions. Coulomb-force control is 3–5 orders of magnitude more fuel-efficient than electric propulsion (EP) methods, and typically requires only a few watts of electrical power to operate [5]. Whereas conventional thrusters can produce a thrust vector pointing in any direction, coulomb forces always lie along the line-of-sight directions between the craft. Further, in space, the spacecraft are not flying in a vacuum, but rather a sparse plasma environment which can shield electrostatic charges. The plasma debye length characterizes the amount of shielding [6,7]. The cold and high-density plasma environment at low earth orbits (LEO) results in

*Graduate Research Assistant, Aerospace Engineering and Sciences Department.
†Associate Professor, Aerospace Engineering and Sciences Department. AIAA Associate Fellow.

centimeter-length debye lengths. This makes the use of coulomb thrusting not feasible at LEO altitudes. However, at geostationary earth orbits (GEO) the debye lengths range between 100–1000 m [5,8], whereas at 1 astronomical unit in deep space they are around 20–40 m [5]. This makes the coulomb thrusting concept feasible for high Earth orbit altitudes and deep-space missions where the maximum separation distances are less than 100 m.

Many promising and challenging applications of coulomb thrusting have been studied. The following papers discuss deep-space (i.e., no orbital motion) coulomb thrusting applications. In [9], Parker et al. present a sequential control strategy for arranging N-charged bodies into an arbitrary geometry using $N + 3$ participating bodies. In [10], Hussein and Schaub study a shape-preserving spinning formation of three spacecraft. Inspired by the gravitational three-body problem, they derive general conditions for open-loop charges that guarantee preservation of the geometric shape of the rotating formation. Parker et al. [11] give an example of an orbit-based coulomb proximity flying mission. Here, a GEO chief satellite deploys deputy craft to specified end states. A multiple-deputy deployment is designed by modulating the control authority across the formation. In [12,13], Natarajan et al. discuss the feedback charge control strategies for the two-craft GEO-based coulomb tether concept. Although these previous studies investigate charge-controlled relative motion between spacecraft, the collision avoidance problem is not directly addressed. Schaub et al. [14] discuss the concept of coulomb thrusting and present a semimajor-axis-based feedback strategy that uses electrostatic forces to bound the motion between two craft. Further, this paper discusses the potential of coulomb thrusting to provide effective collision avoidance strategies, but does not actually develop a control strategy. It discusses the challenges and the potential of this coulomb thrusting application. However, [14] does illustrate numerically that using a simple repulsive force field while at GEO will not guarantee a collision avoidance.

This paper considers the first feedback control strategy using coulomb thrusting to perform collision avoidance maneuvers. A potential collision of two spacecraft flying in deep space is considered where no external forces and torques are acting on the cluster. A charge feedback control strategy is investigated that maintains a desired minimum separation distance between two spacecraft. To minimize the sensor requirements, the control requires only the separation distances and the rates measurements between the craft during the collision avoidance phase. The separation distance is much simpler to measure than the full 6 degree-of-freedom (DOF) relative state vector.

A very simple way to avoid a collision has both spacecraft charged up to large coulomb values with equal sign. The resulting repulsive force drives the craft apart, thus avoiding the collision. But this strategy also results in the two spacecraft flying apart at a considerable velocity, thus noticeably changing their inertial motion. This can cause sensing issues for the spacecraft themselves, but is also of concern if the two craft are operating within a larger cluster of spacecraft. This additional velocity makes future collision avoidance maneuvers more challenging. Instead, the charge feedback control is developed with the additional goal of minimizing changes to the relative kinetic energy level of the two spacecraft.

Finally, the paper also considers the effect of charge saturation on the collision avoidance strategy. Even with sophisticated spacecraft designs, there will always be a physical limit to which a craft can safely be charged. Of interest is determining how much initial approach speed the craft can have and still avoid a collision if the charge levels are limited. Analytical conditions are investigated to guarantee that a collision can be avoided if a given charge limit is considered.

Numerical simulations illustrate the performance of the developed collision avoidance control strategy. These simulations typically consider the craft to be operating in deep space. Although orbiting collision avoidance is not analytically considered in this paper, the numerical simulations do illustrate how the control performs if the spacecraft are not in deep space, but rather in an Earth geostationary orbit.

II. Charged Spacecraft Equations of Motion

Consider two spacecraft flying in the free three-dimensional space where there are no external forces acting on the system, as shown in Fig. 1. In CFF concepts, the electrostatic forces directly control separation distances r_i but not the inertial positions $\mathbf{R}_i$. This paper intends to use the separation distance r and the distance rate $\dot{r}$ as the control feedback, thus the separation distance equations of motion are required to develop the control strategy. The coulomb-force vector between the two spacecraft, acting on m_1, is

$$\mathbf{F} = -k_c \frac{q_1 q_2}{r^3} e^{-\frac{r}{\lambda_d}} \mathbf{r} = -k_c \frac{q_1 q_2}{r^2} e^{-\frac{r}{\lambda_d}} \hat{\mathbf{e}}_r \tag{1}$$

where $k_c = 8.99 \times 10^9 \ \mathrm{C}^{-2} \cdot \mathrm{N} \cdot \mathrm{m}^2$ is the coulomb constant, r is the distance between the two spacecraft, $\mathbf{r}$ is the relative position vector pointing of spacecraft 1 (SC1) to spacecraft 2 (SC2), $\hat{\mathbf{e}}_r$ is the unit vector of $\mathbf{r}$, and λ_d is the debye length. The effective range of a given electrical change is smaller if the plasma debye length is shorter. For high Earth orbits (HEO), the debye length ranges between 100–1000 m [5,8,14]. CFF concepts typically have spacecraft separation distances ranging up to 100 m.

The inertial equations of motion of the two spacecraft are

$$m_1 \ddot{\mathbf{R}}_1 = -k_c \frac{q_1 q_2}{r^2} e^{-\frac{r}{\lambda_d}} \hat{\mathbf{e}}_r \tag{2a}$$

$$m_2 \ddot{\mathbf{R}}_2 = k_c \frac{q_1 q_2}{r^2} e^{-\frac{r}{\lambda_d}} \hat{\mathbf{e}}_r \tag{2b}$$

where $\mathbf{R}_i$ is the inertial position vector of the ith spacecraft. The inertial relative acceleration vector $\ddot{\mathbf{r}}$ is

$$\ddot{\mathbf{r}} = \ddot{\mathbf{R}}_2 - \ddot{\mathbf{R}}_1 = \frac{k_c q_1 q_2}{m_1 m_2 r^2}(m_1 + m_2) e^{-\frac{r}{\lambda_d}} \hat{\mathbf{e}}_r \tag{3}$$

In the kinematics of polar coordinates, the acceleration is given by

$$\ddot{\mathbf{r}} = (\ddot{r} - r\dot{\theta}^2)\hat{\mathbf{e}}_r + (2\dot{r}\dot{\theta} + r\ddot{\theta})\hat{\mathbf{e}}_\theta \tag{4}$$

Substituting Eq. (4) into Eq. (3) yields the scalar separation distance equation of motion:

$$\ddot{r} = r\dot{\theta}^2 + \frac{k_c Q}{m_1 m_2 r^2}(m_1 + m_2) e^{-\frac{r}{\lambda_d}} \tag{5}$$

Note that $2\dot{r}\dot{\theta} + r\ddot{\theta} = 0$ is a consequence of the inertial angular momentum being conserved with coulomb forces. The term $Q = q_1 q_2$ is the charge product between the two spacecraft charges q_i. Because only the separation distance and distance rate will be fed back to the controller, $\dot{\theta}$ should be expressed in terms of r, $\dot{r}$, and the
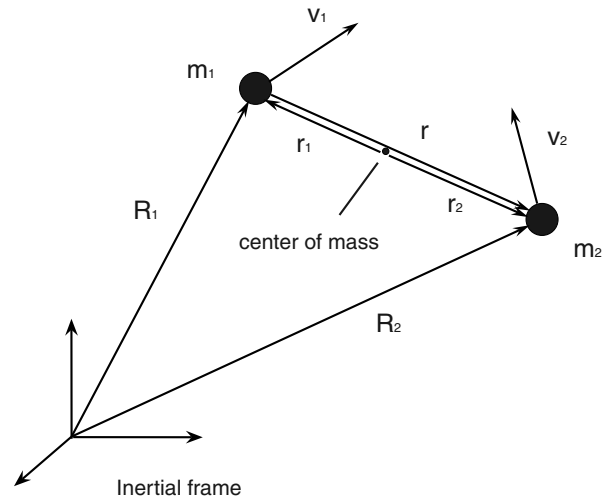

Fig. 1 Illustration of the two-spacecraft system.

initial conditions. This is accomplished by considering the angular momentum about the cluster center of mass.

The position vectors $\mathbf{r}_i$ of the two spacecraft with respect to the center of mass are

$$\mathbf{r}_1 = -\frac{m_2 r}{m_1 + m_2}\hat{\mathbf{e}}_r \tag{6a}$$

$$\mathbf{r}_2 = \frac{m_1 r}{m_1 + m_2}\hat{\mathbf{e}}_r \tag{6b}$$

The angular momentum $\mathbf{H}_c$ of the system about the center of mass is

$$\mathbf{H}_c = \mathbf{r}_1 \times \dot{\mathbf{r}}_1 m_1 + \mathbf{r}_2 \times \dot{\mathbf{r}}_2 m_2 = \frac{m_1 m_2}{m_1 + m_2}r^2\dot{\theta}\hat{\mathbf{e}}_3 \tag{7}$$

Because there are no external torques acting on the system, the momentum vector $\mathbf{H}_c$ is conserved. From $\mathbf{H}_c = \mathbf{H}_c(t_0)$, the angular rate $\dot{\theta}$ is derived

$$\dot{\theta} = \frac{r_o^2}{r^2}\dot{\theta}(t_0) = \frac{r_o}{r^2}\|\dot{\mathbf{r}}(t_0)\|\sin\alpha_0 = \left(\frac{1}{m_1}+\frac{1}{m_2}\right)\frac{\|\mathbf{H}_c(t_0)\|}{r^2} \tag{8}$$

where

$$\alpha_0 = \cos^{-1}\left(\frac{\dot{\mathbf{r}}(t_0)\cdot\mathbf{r}_o}{\|\dot{\mathbf{r}}(t_0)\|r_o}\right)$$

is the angle between $\dot{\mathbf{r}}(t_0)$ and $\mathbf{r}_o$. Thus, the separation distance equation of motion in Eq. (5) is rewritten as

$$\ddot{r} = \left(\frac{1}{m_1}+\frac{1}{m_2}\right)^2\frac{\|H_c(t_0)\|^2}{r^3} + \frac{\beta Q}{r^2}e^{-\frac{r}{\lambda_d}} \tag{9}$$

where

$$\beta = \frac{k_c(m_1+m_2)}{m_1 m_2}$$

The collision avoidance control law challenge is to design the charge product Q such that certain avoidance conditions are satisfied.

III. Unsaturated Control Law

To develop a collision avoidance control law, an explicit statement describing the collision avoidance requirements is needed. Spacecraft 1 (SC1) has a safe region

$$\mathfrak{B}_{r_s} = \{\mathbf{R}\,|\,\|\mathbf{R}-\mathbf{R}_1\| \le r_s\}$$

that can not be penetrated at any time. Each spacecraft is monitoring relative motions of neighboring spacecraft. If another spacecraft (SC2) enters the region

$$\mathfrak{B}_{r_o} = \{\mathbf{R}\,|\,\|\mathbf{R}-\mathbf{R}_1\| \le r_o\}$$

and is flying toward $\mathfrak{B}_{r_s}$, this relative motion is deemed as a potential collision. A control law is then triggered to prevent the potential collision. This paper considers a potential collision of only two spacecraft. Because the radius of the safe region of SC2 can be represented by adding it to the radius of the safe region of SC1, in this paper, SC2 is treated as a point mass moving toward $\mathfrak{B}_{r_s}$ of SC1. Without loss of generality, it is assumed that the initial relative acceleration is zero. This assumption is reasonable because, upon detecting a potential collision, the spacecraft could equalize their charges in preparation for a collision avoidance maneuver.

The chief goals of the control are preventing the potential collision and driving SC2 out of the potential region $\mathfrak{B}_{r_o}$. That is, to keep $r(t) \ge r_s$ for all time and make $r(t) > r_o$ in a finite time. Achievement of the chief goals results in a collision avoidance. On the other hand, it would be undesirable if the final relative kinetic energy level changes too much compared with the original kinetic energy level. The secondary goal of the control design is to maintain the kinetic energy level, that is, to make $\dot{r}_{\text{final}} \approx |\dot{r}(t_0)|$ or to keep the changes bounded. Because only the separation distance is measured, not the full relative states, this condition will only achieve equal radial energy states.

If the trajectory of SC2 does not touch the ball $\mathfrak{B}_{r_s}$, no relative orbit correction is needed to avoid a collision. In this case, the control strategy does not take effect. This situation is illustrated in Fig. 2a. Otherwise, the electrostatic force fields are activated to repel the two spacecraft, as shown in Fig. 2b.

Once SC2 enters $\mathfrak{B}_{r_o}$ and is moving toward $\mathfrak{B}_{r_s}$, the collision avoidance control is triggered to achieve the chief goals and the secondary goal.

A. Lyapunov-Based Control Design

Let us define the state vector $\mathbf{x} = (x_1, x_2)^T$ as

$$x_1 = \begin{cases} r(t)-r_o, & r(t) < r_o \\ 0, & r(t) \ge r_o \end{cases} \tag{10a}$$

$$x_2 = \dot{r}(t) + \dot{r}(t_0) \tag{10b}$$

The state $x_1 = r(t) - r_o < 0$ represents how far SC2 has penetrated into the region $\mathfrak{B}_{r_o}$, and the state $x_2 = \dot{r}(t) + \dot{r}(t_0)$ represents the difference between the expected radial departure rate and the actual distance rate [note that $\dot{r}(t_0) < 0$]. As stated previously, the control law should reduce the absolute values of x_1 and x_2 when $r(t) \le r_o$. When $r(t) > r_o$, a collision avoidance has been achieved. From here on, the control is only trying to make $\dot{r}(t) \to -\dot{r}(t_0)$ to achieve the secondary goal, that is, to maintain the radial relative kinetic energy level. Any final radial separation distance $r_{\text{final}} > r_o$ is acceptable, and is reflected with a zero x_1 state. If the second spacecraft is outside of the region $\mathfrak{B}_{r_o}$ and the radial departure rate is the opposite of the

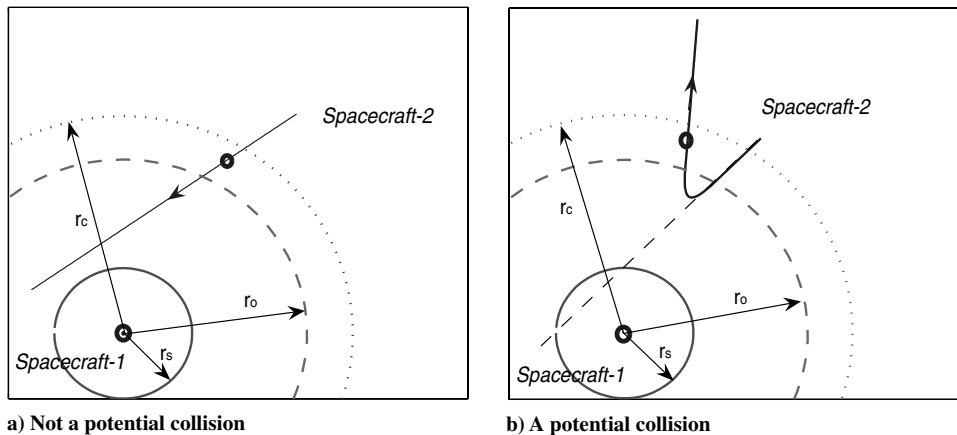a) Not a potential collision

b) A potential collision

Fig. 2   Collision avoidance scenarios as seen by the first spacecraft.

radial approach rate, then both collision avoidance states x_i are zero. Thus, the desired final states are $x_1(t_f) = 0$ and $x_2(t_f) = 0$. To avoid a collision, the safety region penetration variable $x_1(t)$ can never be less than $r_s - r_o$. To achieve this behavior, the Lyapunov function penalizing x_1 is designed to go to infinity when $x_1(t) = r_s - r_o$. Let us define a Lyapunov candidate function as

$$V = \frac{1}{2} k_1 \left(\frac{1}{x_1 - r_s + r_o} - \frac{1}{r_o - r_s} \right)^2 + \frac{1}{2} x_2^2 \quad (11)$$

where k_1 is a constant positive coefficient. This function goes to infinity at the safety boundary $x_1 \to r_s - r_o$ and if the radial separation rate grows unbounded. Note that even though x_1 is defined piecewise, it does not introduce a discontinuity in the Lyapunov function V at $r(t) = r_o$. The first time derivative of the Lyapunov function is

$$\dot{V} = -k_1 \left(\frac{1}{x_1 - r_s + r_o} - \frac{1}{r_o - r_s} \right) \frac{\dot{x}_1}{(x_1 - r_s + r_o)^2} + x_2 \dot{x}_2 \quad (12)$$

Note that here $\dot{x}_2 = \ddot{r}$ as seen from Eq. (10b). The separation distance equation of motion in Eq. (9) relates the charge product Q with $\ddot{r}$. To derive a control law from the Lyapunov function, $\dot{x}_1$ needs to be expressed in terms of the states, system constants, and/or initial conditions. From the definition of x_1 in Eq. (10a), it is obvious that $\dot{x}_1 = x_2 - \dot{r}(t_0)$ when $r(t) < r_o$, but $\dot{x}_1 \neq x_2 - \dot{r}(t_0)$ when $r(t) \geq r_o$.

Note that the term

$$\left(\frac{1}{x_1 - r_s + r_o} - \frac{1}{r_o - r_s} \right)$$

is zero when $r(t) \geq r_o$, so that the first term in Eq. (12) is zero when $r(t) \geq r_o$, no matter what $\dot{x}_1$ is. Thus, $\dot{x}_1$ can be globally replaced with $x_2 - \dot{r}(t_0)$ in the first term of Eq. (12), which simplifies $\dot{V}$ to be

$$\dot{V} = -k_1 \left(\frac{1}{x_1 - r_s + r_o} - \frac{1}{r_o - r_s} \right) \frac{x_2 - \dot{r}(t_0)}{(x_1 - r_s + r_o)^2} + x_2 \ddot{r}(t) \quad (13)$$

Note that $\dot{V}$ is continuous and well defined for all ranges of the separation distance r. Now the separation distance equation of motion in Eq. (9) can be directly substituted into $\dot{V}$ to design a charge feedback control law Q using Lyapunov's direct method.

Assume a charge control law with feedback of separation distance and separation distance rate as

$$Q = \frac{k_1}{\beta} \left(\frac{1}{x_1 - r_s + r_o} - \frac{1}{r_o - r_s} \right) \frac{r(t)^2}{(x_1 - r_s + r_o)^2} e^{\frac{r}{\lambda_d}}$$
$$- \frac{k_2}{\beta} r(t)^2 x_2 e^{\frac{r}{\lambda_d}} \quad (14)$$

Using the Lyapunov function V in Eq. (11), and substituting the charge control in Eq. (14) into the equations of motion in Eq. (9), differentiating V yields the Lyapunov function rate expression:

$$\dot{V} = k_1 \left(\frac{1}{x_1 - r_s + r_o} - \frac{1}{r_o - r_s} \right) \frac{\dot{r}(t_0)}{(x_1 - r_s + r_o)^2}$$
$$- k_2 x_2^2 + x_2 \left(\frac{1}{m_1} + \frac{1}{m_2} \right)^2 \frac{\|\mathbf{H}_c\|^2}{r^3} \quad (15)$$

Note that

$$\left(\frac{1}{x_1 - r_s + r_o} - \frac{1}{r_o - r_s} \right) \geq 0$$

and equals zero when $x_1 = 0$. Because $\dot{r}(t_0) < 0$, the first term in Eq. (15) cannot be positive. Thus, the Lyapunov function rate is bounded by

$$\dot{V} \leq -k_2 x_2^2 + x_2 \left(\frac{1}{m_1} + \frac{1}{m_2} \right)^2 \frac{\|\mathbf{H}_c\|^2}{r^3} \quad (16)$$

Let the function $b(r)$ be defined as

$$b(r) = \frac{1}{k_2} \left(\frac{1}{m_1} + \frac{1}{m_2} \right)^2 \frac{\|\mathbf{H}_c\|^2}{r^3} > 0 \quad (17)$$

Note that $b(r) \to 0$ as $r \to \infty$. Because $b(r) > 0$, Eq. (16) shows that $\dot{V} < 0$ if

$$x_2 > b(r) \quad \text{or} \quad x_2 < 0 \quad (18)$$

The $\dot{V}$ expression in Eq. (16) does not yet yield any stability guarantees. Initial conditions for $\dot{V} < 0$ must be determined.

B. State Convergence and Collision Avoidance Achievement

Next, the stability and convergence of the charge control law in Eq. (14) is discussed. A collision avoidance should result in $r(t) > r_s$, while a secondary goal attempts to drive $x_2 \to 0$.

Theorem 1: For a two-body system with equations of motion as shown in Eq. (2), the charge control law in Eq. (14) makes the state x_2 converge to the interval $[0, b(r)]$. Further, assuming $x_1 \to 0$ in a finite time, x_2 converges either to zero or to $b(r)$ as $t \to \infty$.

Proof: Eq. (18) shows that $\dot{V} < 0$ if x_2 is outside of the interval $[0, b(r)]$. According to the Lyapunov stability theory, the charge control law in Eq. (14) will drive $\dot{V}$ to zero. Thus, $x_2 \to [0, b(r)]$ asymptotically as $t \to \infty$.

By the assumption that $x_1 \to 0$ in a finite time $t^\dagger$, the inequality in Eq. (16) becomes an equality for $t \geq t^\dagger$. Then, $\dot{V} > 0$ when $x_2 \in (0, b(r))$, and $\dot{V} = 0$ when $x_2 = 0$ or $x_2 = b(r)$ for $t \geq t^\dagger$. According to the Lyapunov stability theory, x_2 will be driven to zero or $b(r)$. So x_2 converges either to zero or to $b(r)$ as $t \to \infty$.□

Theorem 2: Assuming a two-body system, with the dynamics described by Eq. (2), is subjected to the charge control law in Eq. (14), then the states $(x_1, x_2) \to (0, 0)$ as $t \to \infty$, where x_1, x_2 are defined by Eq. (10).

Proof: Theorem 1 guarantees that $x_2 \to [0, b(r)]$ as $t \to \infty$. The relationship between x_2 and $\dot{r}$ in Eq. (10b) indicates that $\dot{r} \to [-\dot{r}(t_0), b(r) - \dot{r}(t_0)]$. Because $\dot{r}(t_0) < 0$, $\dot{r}$ will become a strictly positive value at a finite time t^+. As a result, at time $t^* > t^+$ the separation distance reaches the outer collision avoidance distance r_o, and for $t > t^*$, $r(t) > r_o$. Referring to the definition of x_1 in Eq. (10), it can be concluded that $x_1 \to 0$ in a finite time. Because of $\dot{r}$ being strictly positive, the separation distance $r \to \infty$ as $t \to \infty$.

Having shown that the two spacecraft will depart the collision avoidance region, next, the convergence of x_2 is investigated as $t \to \infty$. If $\mathbf{H}_c = 0$, the interval $[0, b(r)]$ becomes the zero point. Thus, $x_2 \to 0$ due to the Theorem 1 property $x_2 \to [0, b(r)]$. For the case in which $\mathbf{H}_c \neq 0$, the properties of x_2 need to be further investigated. The definition in Eq. (10b) yields $x_2(t_0) = 2\dot{r}(t_0) < 0$. Here x_2 will either converge to zero or to $b(r)$ because $x_1 \to 0$ in a finite time has been proven. If x_2 never reaches zero, then $x_2 \to 0$. If x_2 crosses zero and converges to $b(r)$, then $x_2 \to 0$ due to $b(r) \to 0$. □

Theorem 3: For a two-body system with dynamics described by Eq. (2), the charge product control law in Eq. (14) prevents any potential collision by keeping $r(t) > r_s$ for all time, and making $r(t) > r_o$ in a finite time.

Proof: While proving $x_1 \to 0$ in Theorem 2, it has been shown that $r(t) > r_o$ is true for $t > t^*$. Thus, the condition $r(t) \geq r_s$ for all time is left to be proven. Note that $r(t)$ starts with $r_o > r_s$. The definitions of V in Eq. (13) and x_1 in Eq. (10a) show that $V \to \infty$ if and only if $r(t)$ decreases to be r_s or $x_2 \to \infty$. Theorem 1 shows that $x_2 \not\to \infty$. Thus, to prove $r(t) > r_s$ for all time, it is equivalent to prove that $V \not\to \infty$ for all time.

The inequality in Eq. (16) shows that the only chance for $\dot{V}$ to be positive is $x_2 \in (0, b(r))$. Thus, a necessary but not sufficient condition for $V \to \infty$ is that x_2 stays in $(0, b(r))$ for an infinite time. But, as mentioned, while proving Theorem 2, $r(t)$ is increasing as

$x_2 \in (0, b(r))$. Because x_1 increases as $r(t)$ increases, x_1 does not decrease to $r_o - r_s$ when $x_2 \in (0, b(r))$. The definition of V in Eq. (11) shows that V is bounded when $x_2 \in (0, b(r))$ and $x_1 > r_o - r_s$. Thus, even when $x_2 \in (0, b(r))$ for an infinite time, V is still bounded. So $V \nrightarrow \infty$ is guaranteed for all time, hence $r(t) > r_s$ is true for all time. □

Practically speaking, the range of the electrostatic control is limited due to the drop off of the coulomb field strength with increasing separation distances. As a result, the controller will be turned off after the state goes inside a certain dead-zone region. Let us define a radius $r_c > r_o$ where the collision avoidance charge control is turned off. The effect of this limitation is a termination of the control when $x_1 = 0$ and $r(t) > r_c$. Note that when the truncation happens, the potential collision has been avoided. After the control charges are turned off, there are no forces acting on the spacecraft. The two spacecraft are now flying freely in space (with the assumption that the spacecraft are flying in free space) with constant velocities. The separation distance rate is still bounded, even though it is not converging to the magnitude of the approach rate.

Given the charge product in Eq. (14) to produce the required electrostatic force field, the individual spacecraft charges q_i are evaluated through

$$q_1 = \sqrt{|Q|} \tag{19}$$

$$q_2 = \text{sgn}\,(Q)q_1 \tag{20}$$

There is an infinity number of choices for how Q can be mapped into q_1 and q_2. This strategy evenly distributes the charge amount across both craft. If one spacecraft can handle a higher charge level than the other spacecraft, adding a coefficient can adjust the charge distribution.

IV. Saturated Collision Avoidance Analysis

Without the saturations of the spacecraft charges, the controller presented in the previous section can always prevent a potential collision. But, in reality, the spacecraft charge magnitudes are always limited. The ability of the two-body system to prevent a potential collision is reduced compared with the nonsaturated control law. If the spacecraft are moving fast enough, then a collision cannot be avoided with a limited force. Hence, for a given pair of limited charges, collision avoidance cannot be guaranteed for all initial conditions.

This section discusses limited charge control requirements for a collision to be preventable. Assume the two spacecraft are fully charged such that the charge product reaches its maximum positive value. If the separation distance r still decreases to be less than the safety-restraint distance r_s, the potential collision is deemed as not avoidable. Otherwise, the potential collision is avoidable.

A. Constant Charge Spacecraft Equations of Motion

Our discussion of the conditions for a potential collision to be avoidable is based on the assumption that the charge product remains at its maximum value $Q = Q_{\max} > 0$ to generate the largest repulsive force. The coulomb-force expression in Eq. (1) simplifies to

$$\mathbf{F} = -k_c \frac{Q_{\max}}{r^3} e^{-\frac{r}{\lambda_d}} \mathbf{r} \tag{21}$$

and the differential relative equation of motion is

$$\ddot{\mathbf{r}} = \beta \frac{Q_{\max}}{r^3} e^{-\frac{r}{\lambda_d}} \mathbf{r} \tag{22}$$

Note that the form of the coulomb force is very similar to the gravity force; this makes it possible to describe the motion using the formulas of the gravitational two-body problem (2BP). Hussein and Schaub [10] provide an approach to analyze this coulomb-forced spacecraft motion using the 2BP method. To apply a 2BP method in analyzing the coulomb-forced motion, it is necessary to find the

radius and the energy equation in a similar form as in the 2BP. Let us introduce the effective gravitational parameter

$$\mu(r) = -k_c \frac{Q_{\max}(m_1 + m_2)}{m_1 m_2} e^{-\frac{r}{\lambda_d}} \tag{23}$$

Next, assume that $r \ll \lambda_d$, which means the plasma shielding effect is weak. Then $e^{-r/\lambda_d} = 1$ and the parameter $\mu(r)$ becomes a constant

$$\mu = -k_c \frac{Q_{\max}(m_1 + m_2)}{m_1 m_2} \tag{24}$$

The relative equations of motion reduce to the familiar 2BP form

$$\ddot{\mathbf{r}} = -\frac{\mu}{r^3} \mathbf{r} \tag{25}$$

Equation (25) has the same form as the equation of motion of the gravitational 2BP, except that here μ is a negative number because $Q_{\max} > 0$. By assuming $r \ll \lambda_d$, μ becomes a constant, and so the orbit radial trajectory is a conic section curve. Because $\mu < 0$ for the repulsive force case, all relative trajectories are hyperbolas where craft 2 orbits the farther focus [10]. The signs of some parameters of the conic section are different from that of the gravitational 2BP. In our case, $\mu < 0$, the semilatus radium $p < 0$ and the semimajor axis $a > 0$.

Because the repulsive hyperbolic motion has the craft orbit about an unoccupied focal point, the radial equation is different from that of the gravitational 2BP [10]:

$$r = \frac{p}{1 - e \cos f} \tag{26}$$

Here, the semilatus rectum $p = h^2 \mu < 0$, and h is the magnitude of the specific angular momentum $\mathbf{h} = \mathbf{r} \times \dot{\mathbf{r}}$. The energy equation is derived in the same procedure as the 2BP, and yields an identical equation:

$$\frac{v^2}{2} - \frac{\mu}{r} = -\frac{\mu}{2a} \tag{27}$$

where v is the magnitude of velocity vector $\dot{\mathbf{r}}$

$$v^2 = \dot{\mathbf{r}} \cdot \dot{\mathbf{r}} = \dot{r}^2 + (r\dot{f})^2 = \dot{r}^2 + \frac{h^2}{r^2} \tag{28}$$

and $\dot{f}$ is the in-plane rotation rate.

Because the total energy is positive, the relative trajectory of the two spacecraft is a hyperbola. As seen by SC1, SC2 is traveling along the hyperbola, and SC1 is standing at the farther focus point [10], as illustrated in Fig. 3.

From Eq. (26), the closest separation distance corresponds to the distance when $f = 0$, that is, the radius of periapsis
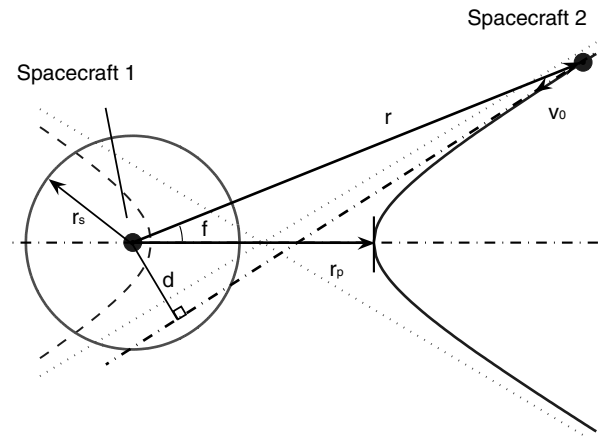

Fig. 3 Illustration of the two-body hyperbolic trajectory.

$$r_p = \frac{p}{1-e} = a(1+e) \tag{29}$$

Thus, given an initial spacecraft approaching speed, finding the criterion for a collision avoidance is to determine a required saturated charge level that guarantees

$$r_p \geq r_s \tag{30}$$

B. Avoidance Analysis

When the specific angular momentum satisfies $\mathbf{h} \neq 0$, there exists an offset distance d between the position of SC1 and the direction of the relative velocity of SC2, as shown in Fig. 3. Note that here it is assumed that the current flight path will result in a potential collision where r will become less than r_s. The specific angular momentum is represented in terms of d and v_0:

$$h = \|\mathbf{r}_o \times \dot{\mathbf{r}}(t_0)\| = d v_0 \tag{31}$$

The parameter h is expressed in terms of v_0 and d instead of the $\dot{r}(t_0)$ and $\dot{f}_0$ set, because it will be easier to find out the criterion of v_0. Assume that $r(t)$, $\dot{r}(t)$, and f can be measured, v_0 and d are calculated through

$$v_0 = \sqrt{\dot{r}(t_0)^2 + (r_o \dot{f}_0)^2} \tag{32}$$

$$d = \frac{r_o^2 \dot{f}_0}{v_0} \tag{33}$$

Because the angular momentum is conserved during the electrostatic collision avoidance maneuver, as with the 2BP, the relationship between the angular momentum and the orbit elements is

$$h^2 = \mu a(1 - e^2) \tag{34}$$

Solving for the eccentricity e yields

$$e = \sqrt{1 - \frac{h^2}{\mu a}} \tag{35}$$

This e formulation can be used to calculate the periapsis radius r_p:

$$r_p = a(1+e) = a + \sqrt{a^2 - \frac{ah^2}{\mu}} \tag{36}$$

The collision avoidance criterion $r_p \geq r_s$ yields the condition

$$a + \sqrt{a^2 - \frac{ah^2}{\mu}} \geq r_s \tag{37}$$

Subtracting a from both sides and squaring the result yields

$$-\frac{ah^2}{\mu} \geq r_s^2 - 2ar_s \tag{38}$$

Now, the semimajor axis a is needed to obtain the relationship between μ and the initial states of the system. From the energy equation in Eq. (27), a is solved as

$$a = \frac{r_o \mu}{2\mu - r_o v_0^2} \tag{39}$$

Substituting Eq. (39) into Eq. (38), and using $h = v_0 d$, yields

$$-\frac{r_o v_0^2 d^2}{2\mu - r_o v_0^2} \geq r_s^2 - \frac{2r_o r_s \mu}{2\mu - r_o v_0^2} \tag{40}$$

Note that $2\mu - r_o v_0^2 < 0$. Multiplying both sides by $-(2\mu - r_o v_0^2)$ results in

$$r_o v_0^2 d^2 \geq r_s^2 r_o v_0^2 + 2r_s(r_o - r_s)\mu \tag{41}$$

Equation (41) shows the relationship of d, v_0, and μ for an avoidable collision. Solving Eq. (41) for μ, and using the definition of μ in Eq. (24), yields the maximum required charge criterion to avoid a collision with a given initial approach speed v_0 and miss-distance d.

$$Q_{\max} \geq \frac{m_1 m_2}{m_1 + m_2} \frac{r_o v_0^2 (r_s^2 - d^2)}{2k_c r_s (r_o - r_s)} \tag{42}$$

For example, a large value of $\dot{r}(t_0)^2$ means SC2 is approaching SC1 at a high speed. Here, v_0 is large, and according to Eq. (42), a large $Q_{\max}$ is required to avoid the collision. If the upper limit of the initial separation distance rate $\dot{r}(t_0)$ is known, then Eq. (42) tells us the minimum value of the saturated charge product needed to avoid the collision. For a given formation flying mission in which the maximum magnitude of the possible separation distance rate has been determined, Eq. (42) helps us design the electric charge devices of the coulomb-forced spacecraft to provide the maximum required repulsive forces.

Alternatively, solving Eq. (41) for v_0 yields the criterion for the magnitude of the relative velocity:

$$v_0 \leq \sqrt{\frac{2\mu r_s(r_o - r_s)}{r_o(d^2 - r_s^2)}} \tag{43}$$

If the parameter μ of the spacecraft is given (specifically, maximum spacecraft charge), then Eq. (43) tells us the maximum allowable relative velocity that guarantees the collision to be avoidable. As expected, the smaller the allowable charge levels, the smaller are the allowable approach speeds v_0.

To provide insight into the relationship between the maximum charge and initial velocity, Fig. 4 shows the critical surface of parameters d, v_0, and $Q_{\max}$ under the following conditions:

$$\begin{cases} m_1 = 50 \text{ kg} \\ m_2 = 50 \text{ kg} \end{cases}, \quad \begin{cases} r_s = 4 \text{ m} \\ r_o = 18 \text{ m} \end{cases} \tag{44}$$

Parameters d, v_0, and $Q_{\max}$ in the region above the critical surface represent avoidable collisions. Beneath the surface are parameters of unavoidable collisions.

This critical surface is one-quarter of a saddle surface. When the magnitude of the relative velocity v_0 is set, if the offset distance d is large, then a small value of $Q_{\max}$ is required to prevent the collision. And when $d = r_s$, $Q_{\max} = 0$, the trajectory of SC2 will touch the safe region of SC1 $\mathfrak{B}_{r_s}$ but will not penetrate it without any control. If the offset distance d is set, a larger v_0 results in the bigger $\dot{r}_0$ component,
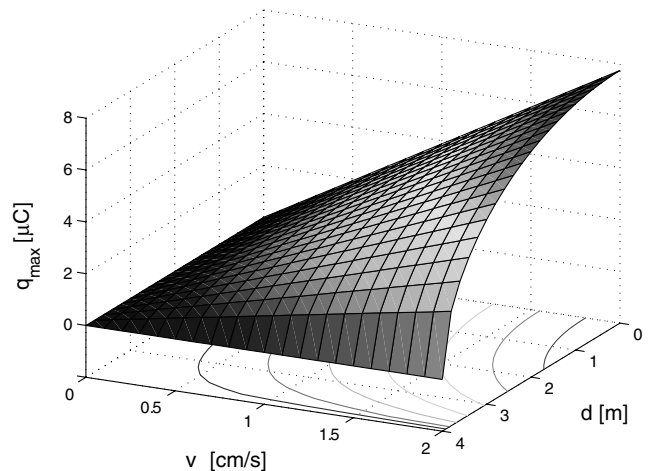

Fig. 4 Critical surface of parameters for an avoidable collision.

thus a larger Q_{max} is required for a collision avoidance maneuver. When $v_0 = 0$, which means the two spacecraft are stationary to each other, nothing needs to be done to avoid a collision, and so Q_{max} in this case remains zero.

When $h = 0$, then the offset distance $d = 0$ and the spacecraft are lined up for a head-on collision. For this worst case situation, the criteria in Eq. (42) and Eq. (43) reduce to

$$Q_{max} \geq \frac{\dot{r}(t_0)^2}{2k_c} \frac{m_1 m_2}{m_1 + m_2} \frac{r_o r_s}{r_o - r_s} \tag{45}$$

$$\dot{r}(t_0)^2 \leq 2\mu \left(\frac{1}{r_o} - \frac{1}{r_s} \right) \tag{46}$$

Note that even though the derivation of the criteria is based on the assumption that $Q = Q_{max} > 0$ and $d < r_s$, the same procedure can also be performed in the case $Q = Q_{min} < 0$ and $d > r_s$. In this case, the two spacecraft are attracting each other. The problem is then changed to analyzing the requirements to prevent the two attracting spacecraft from colliding. Following the same procedure in deriving the criterion in Eq. (42), yields

$$Q_{min} \geq \frac{m_1 m_2}{m_1 + m_2} \frac{r_o v_0^2 (r_s^2 - d^2)}{2k_c r_s (r_o - r_s)} \overset{\text{def}}{=} g \tag{47}$$

Equation (47) has exactly the same form as Eq. (42). Because $d > r_s$, here $g < 0$. It is assumed that the two spacecraft are attracting each other, and so the charge product Q is always negative. The smaller Q is, the larger the attracting force becomes, and thus the more likely the two spacecraft will get closer. If, in a mission, the two spacecraft are fully charged such that $Q = Q_{min}$, then Eq. (47) tells us the minimum allowable value of the limit of the negative charge product Q, guaranteeing that the spacecraft will not collide.

V. Numerical Simulations

While the charge control is derived for the general three-dimensional spacecraft motion, the conservation of angular momentum forces all resulting motion to be planar. Thus, without loss of generality, the following numerical simulations all consider planar motion to simplify the visualizations.

The masses of the two spacecraft are $m_1 = m_2 = 50$ kg. At first, let us assume that the spacecraft are flying in deep space with the debye length being $\lambda_d = 50$ m. The radii of the safe region r_s and the potential region r_o are determined by the requirements of a specific formation mission. For these simulations, r_s and r_o are set as

$$r_s = 3 \text{ m}, \qquad r_o = 16 \text{ m}$$

The region of the effective control range r_c will be given in specific simulation examples. The initial inertial coordinates and inertial velocities are

$$\begin{cases} \mathbf{R}_1 = [-8, -3]^T \text{ m} \\ \mathbf{R}_2 = [8, 3]^T \text{ m} \end{cases}, \quad \begin{cases} \dot{\mathbf{R}}_1 = [0.006 \, 0.002]^T \text{ m/s} \\ \dot{\mathbf{R}}_2 = [-0.006 \, -0.002]^T \text{ m/s} \end{cases} \tag{48}$$

These initial conditions are set up such that the spacecraft cluster's center of mass is stationary.

A. Simulation Without Control Truncation or Charge Saturations

The unsaturated charge control law in Eq. (14) is guaranteed to prevent any collision. As to the coefficients of the controller, the larger k_1 is, the more the spacecraft proximity near r_s is penalized. A larger k_2 results in more control effort in driving $\dot{r} \to -\dot{r}(t_0)$. For the first simulation, the controller coefficients are chosen as

$$k_1 = 0.000001 \text{ kgm}^4\text{s/C}^2, \qquad k_2 = 0.0002 \text{ s/C} \tag{49}$$

These coefficients result in a case in which the state x_2 crosses zero and then converges to $b(r)$. Figure 5 shows the numerical simulation

results with the initial conditions listed previously. Note that, here, the effective control range r_c is set to be infinity and no control truncation is occurring. The SC1 and SC2 start from a separation distance slightly larger than r_o. Before $r(t) = r_o$, the control is not triggered and the charges remain zeros. When $r(t) = r_o$, the control is triggered and the spacecraft start to repel each other. After about 1.3 h, it is found that $r(t) > r_o$, and the control law is now only trying to equalize the radial separation rate magnitude to the initial value. The collision has already been avoided at this time. The following discussion illustrates the analytical predictions of the behaviors of x_2.

From Theorem 1, x_2 converges to the interval $[0, b(r)]$. Further, it eventually converges to $b(r)$ if it crosses zero. Figures 5d and 5e show the histories of the separation distance rate for different time spans. After x_2 crosses zero, it keeps rising up as predicted. Figure 5e shows that x_2 crosses $b(r)$ at point A. At this critical point, $\dot{V} = 0$ and $x_2 = b(r) > 0$. Using Eq. (14), the charge product can be solved as

$$Q = -\frac{\|\mathbf{H}_c\|^2}{k_c r} e^{\frac{r}{\lambda_d}} \tag{50}$$

From the separation distance equation of motion in Eq. (9), we find that the acceleration of the separation distance is $\ddot{r} = 0$. Note that $\dot{x}_2 = \ddot{r}$, thus x_2 stops increasing at point A, and starts to decrease. At point A, $\dot{x}_2 = 0$, and x_2 is bounded by b function value at point A. So x_2 crosses the history of $b(r)$ because $b(r)$ is decreasing. After x_2 hits $b(r)$, it converges to the trajectory of $b(r)$ asymptotically because $\dot{V} < 0$.

Figure 5f shows that after 15 h, the spacecraft start to attract each other to make x_2 to converge to $b(r)$. As shown in Fig. 5e, this is when the state x_2 becomes positive. Physically, $x_2 > 0$ means that the separation rate is now larger than the original radial approach rate magnitude. To slow down the radial motion, the signs of the charges become opposite to yield attractive forces. The reason the magnitudes of the charges are increasing here is that the separation distance has already grown very large. Even though the required control force is very small, the $1/r^2$ dependency of the coulomb-force expression requires a large spacecraft charge to generate it. This issue has little to no practical consequence because the collision avoidance maneuver was effectively finished after about 1.3 h. This long-term behavior is illustrated to provide a numerical example of the analytically predicted behaviors of x_2.

When the controller's coefficients are set to be the preceding values

$$k_1 = 0.0002 \text{ kgm}^4\text{s/C}^2, \qquad k_2 = 0.0001 \text{ s/C} \tag{51}$$

With these parameters, the state x_2 does not reach zero, as seen in the simulation results in Fig. 6. But x_2 still converges asymptotically to zero from a negative value. As shown in Fig. 6d, because k_1 is large, the control charges that penalize the spacecraft proximity near r_s dominate in the initial 1 h. The first peak of the charge product happens when the two spacecraft get closest. Physically, when the craft get close, the repulsive force suddenly increases to a peak to repel the craft. This results in a sharp trajectory of the spacecraft, as shown in Fig. 6a.

B. Simulation with Charge Truncations

In the following simulations, the control is truncated when the separation distance is larger than r_c where $r_c > r_o$. The range of the control is denoted by $\mathfrak{B}_{r_c}$ with radius r_c. The control charges are turned off when the separation distance $r(t) > r_c$. Setting $r_c = 20$ m, and the controller's coefficients

$$k_1 = 0.0001 \text{ kgm}^4\text{s/C}^2, \qquad k_2 = 0.0003 \text{ s/C} \tag{52}$$

and using the previous spacecraft initial position and velocity conditions, yields Fig. 7 which shows the simulation results in this case.

Because of the charge truncations, x_2 is not guaranteed to converge to zero during this maneuver. However, as the control analysis predicts, the radial rate tracking error x_2 will remain

a) Inertial scenario

b) Scenario as seen from SC1

c) Separation distance history

d) Separation distance rate

e) Illustration of the convergence of x_2 to $b(r)$
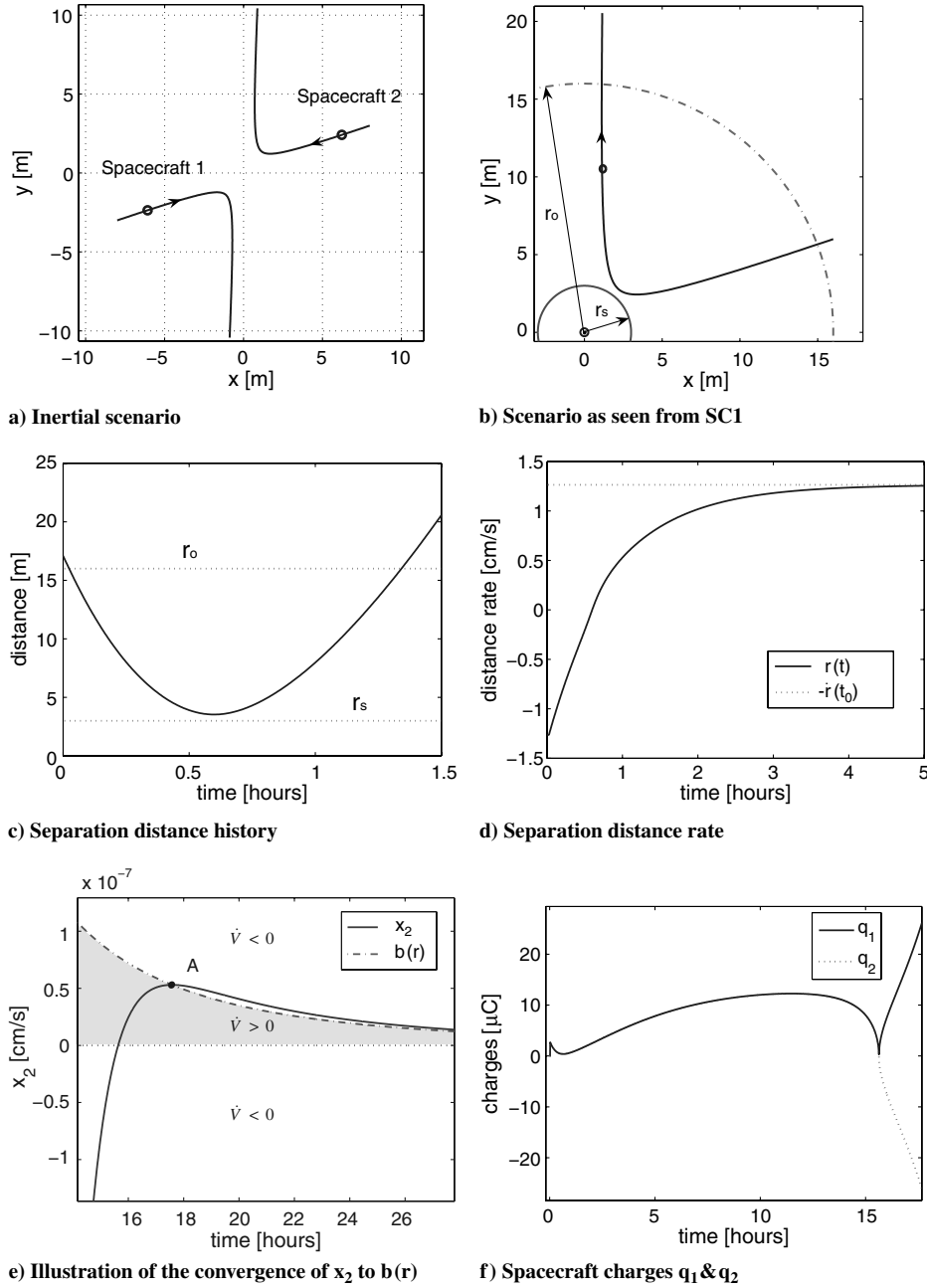

f) Spacecraft charges q_1 & q_2

Fig. 5   Simulation results without truncation and charge saturations, in the case that x_2 crosses zero.

bounded while achieving a collision avoidance maneuver where $x_1 \rightarrow 0$.

To test the robustness of the control, the spacecraft are put in an geostationary orbit to compare the performance with that of the spacecraft flying in deep space. The initial conditions in Eq. (48) are treated as LVLH (local vertical local horizontal) frame position and velocity vectors, which are then mapped into inertial vectors with respect to the Earth-centered inertial frame. The full nonlinear equations of motion are then integrated with the same charge collision avoidance control applied. After the integration, the resulting motion is mapped back into equivalent LVLH frame position vectors, where the rotating LVLH frame is assumed to be the spacecraft cluster's center of mass. The simulation results are illustrated in Fig. 7 simultaneously with the simulation performed in deep space.

The parameters of the two spacecraft and the controller are kept unchanged to the truncated control example. In GEO the debye length ranges from 100–1000 m. But, for a fair comparison, here the debye length is still set to be $\lambda_d = 50$ m. Although the trajectories in

Fig. 7a are different for deep space and GEO cases, they both yield a separation distance $r(t)$ that is always greater than the safety limit r_s. From the charge control law in Eq. (14), the charge product Q will increase if $r(t)$ gets too close to r_s. In fact, $Q \rightarrow \infty$ if $r(t) \rightarrow r_s$. Thus, although the orbital motion is not analyzed explicitly in this study, if the collision avoidance happens quickly enough as compared with the orbital dynamics, the algorithm can still be effective.
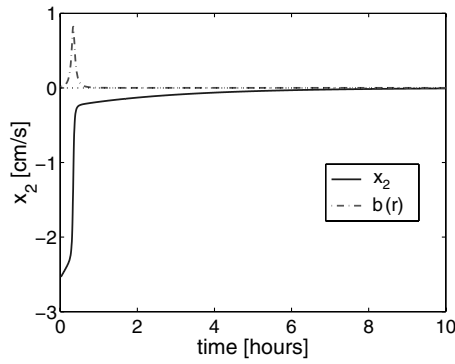
C.   Simulation with Charge Saturations

When the spacecraft charge saturations are introduced, a potential collision is unpreventable if the two spacecraft are flying toward each other at a very high speed. Equations (42) and (43) provide the criteria for an avoidable potential collision. Note that, even though the analysis of the criteria is based on the assumption that the debye length $\lambda_d \rightarrow \infty$, the following numerical simulation still has the debye length set to $\lambda_d = 50$ m to show how close the simplified charge limit estimation in Eq. (42) is with that of a more complex
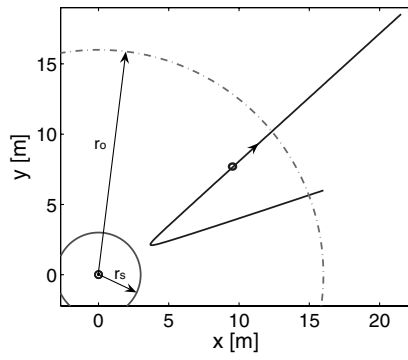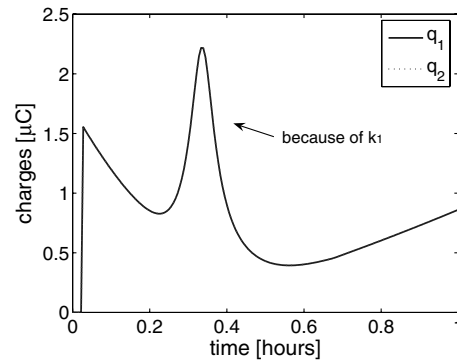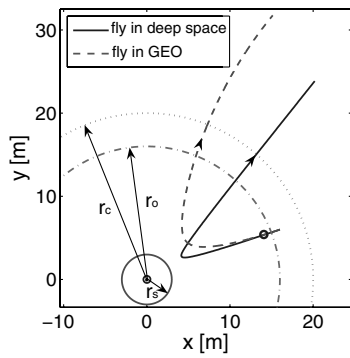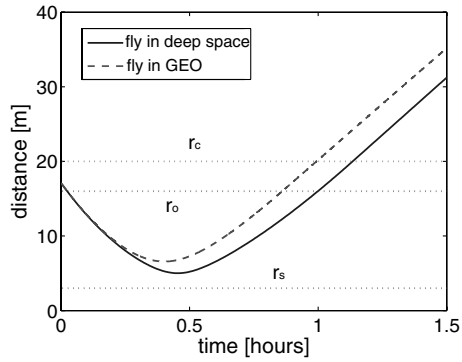
a) Scenario as seen from SC1
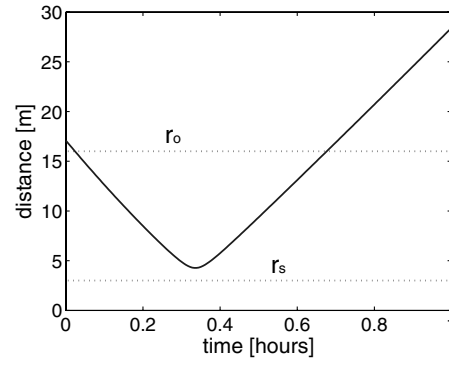
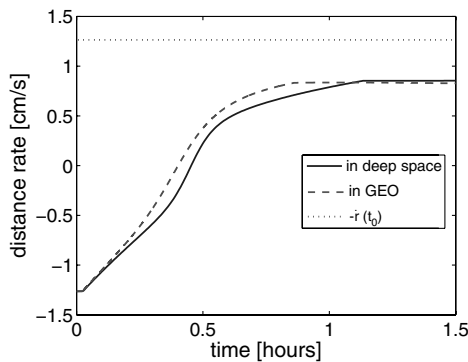b) History of the separation distance

c) History of the separation distance rate

d) History of charges q_1

Fig. 6   Simulation results without truncation and charge saturations, in the case that x_2 will not cross zero.

a) Scenario as seen from SC1

b) History of the separation distance
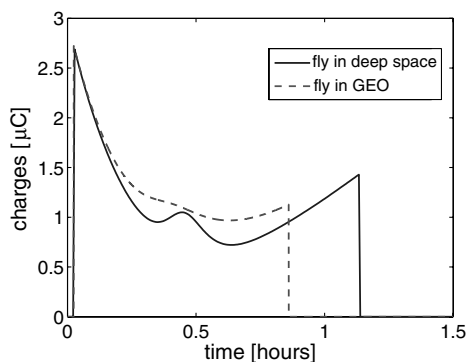

c) History of the separation distance rate

d) History of charges q_1

Fig. 7   Simulation results with truncation but without charge saturations.

a) Scenario as seen from SC1

b) History of the separation distance

c) History of the separation distance rate
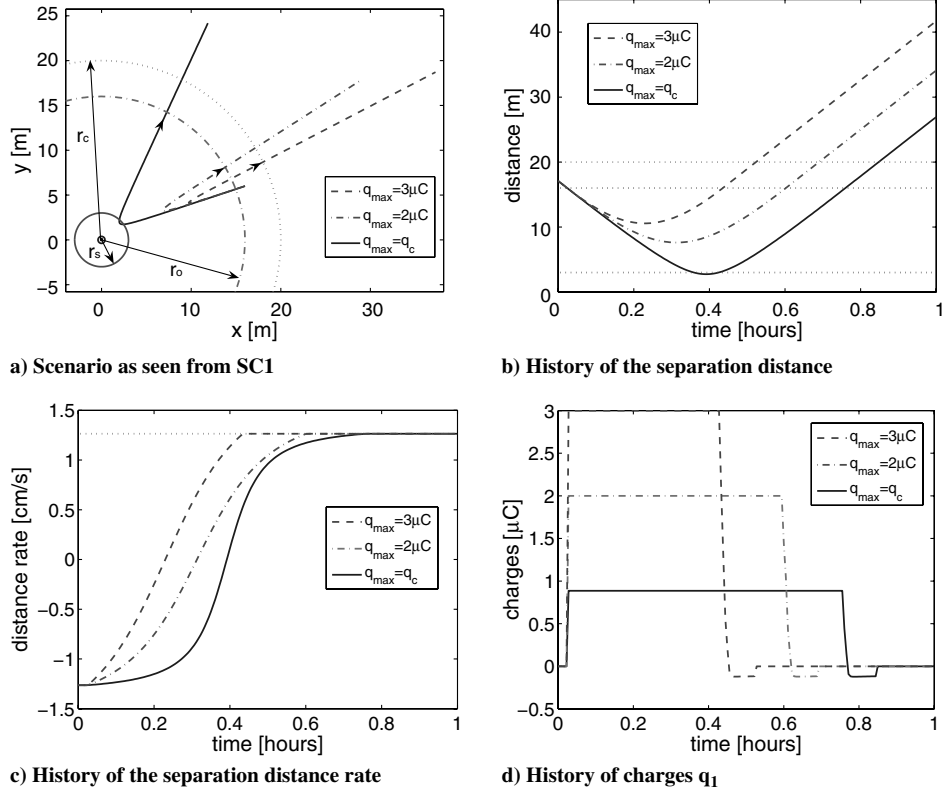
d) History of charges q_1

Fig. 8   Simulation results with charge saturation.

motion with a limited debye length. With the same initial conditions as in the previous simulation examples in Eq. (48), the initial offset distance d and the magnitude of initial relative velocity v_0 are

$$d = 0.6325 \text{ m}, \qquad v_0 = 0.0126 \text{ m/s}$$

Using r_s, r_o, and masses m_i, the critical charge product for an avoidable collision is

$$Q_C = \frac{m_1 m_2}{m_1 + m_2} \frac{r_o v_0^2 (r_s^2 - d^2)}{2 k_c r_s (r_o - r_s)} = 7.8492 \times 10^{-13} \text{ C}^2 \qquad (53)$$

The critical saturation limit for each individual charge is $q_c = \sqrt{Q_C} = 0.88596 \ \mu\text{C}$.

Figure 8 shows simulation results with the same initial conditions but different charge saturation limits. It is assumed that, in the potential region $\mathfrak{B}_{r_o}$, the two spacecraft are fully charged to repel each other. This can be achieved by setting the controller's coefficients k_1 and k_2 to be some large numbers. Here, the controller's parameters are set to be

$$k_1 = 0.1 \text{ kgm}^4\text{s/C}^2, \qquad k_2 = 0.1 \text{ s/C} \qquad (54)$$

It can be seen that a larger q_{max} results in a more aggressive repulsion with a larger periapses radius. When $q_{max} = q_c$, the closest distance is slightly smaller than r_s. SC2 penetrates about 0.25 m inside the safe restraint region $\mathfrak{B}_{r_s}$ with $r_s = 3$ m. This happens because the debye length effect partially shields the electrostatic force between the spacecraft. Note that in real space missions, r_s is a safety-restraint distance estimate that guarantees no physical contact happens and the electrical devices on both spacecraft will not interfere with each other. The 0.25 m's penetration is not large when compared with r_s, at only about 8%. On the other hand, if we know how much debye shielding will occur, the value of r_s can be adjusted to be larger, such that the closest distance between the spacecraft is still big enough to keep the spacecraft and all the devices safe. At this point, it can be concluded that the estimation of the charge product criterion in Eq. (42) is sufficiently good to provide a practical maximum required charge computation.

VI.   Conclusions

A coulomb-force-based collision avoidance control problem of two spacecraft is discussed. After formulating the equation of motion of the separation distance, a collision avoidance charge control law with the feedback of the separation distance and the distance rate is developed based on Lyapunov's direct method. Without saturation and truncation of the spacecraft charges, the control is able to prevent collisions while keeping the final kinetic energy the same as the initial kinetic energy. The charge truncation introduces an uncertainty in maintaining the relative kinetic energy, but the collision avoidance purpose is still achieved and the change in kinetic energy is guaranteed to be bounded. The charge saturation may lead to a failure in achieving a collision avoidance. Analytical conditions for a preventable collision are formulated by ignoring the plasma shielding effect. Simulations show that the predicted minimum separation distance obtained using the analytical criteria is close to the actual minimum distance when the plasma shielding effect is taken into account, thus the criteria are practically usable.

Acknowledgments

References

[1] Slater, G. L., Byram, S. M., and Williams, T. W., "Collision Avoidance for Satellites in Formation Flight," *Journal of Guidance, Control, and Dynamics*, Vol. 29, No. 5, Sept.–Oct. 2006, pp. 1140–1146.

[2] Singh, G., and Hadaegh, F. Y., "Collision Avoidance Guidance for Formation-Flying Applications," *AIAA Guidance, Navigation, and Control Conference and Exhibit*, AIAA Paper 2001-4088, 2001.

[3] Campbell, M. E., and Udrea, B., "Collision Avoidance in Satellite Clusters," *Proceedings of the 2002 American Control Conference*, Vol. 2, Inst. of Electrical and Electronics Engineers, New York, 2002, pp. 1686–1692.

[4] Scharf, D. P., Acikmese, A. B., Ploen, S. R., and Hadaegh, F. Y., "Direct Solution for Fuel-Optimal Reactive Collision Avoidance of Collaborating Spacecraft," *Proceedings of the 2006 American Control Conference*, Inst. of Electrical and Electronics Engineers, New York, 2006, p. 6.

[5] King, L. B., Parker, G. G., Deshmukh, S., and Chong, J.-H., "Spacecraft Formation-Flying Using Inter-Vehicle Coulomb Forces," NASA Inst. for Advanced Concepts Technical Rept., Jan. 2002, http://www.niac.usra.edu.

[6] Nicholson, D. R., *Introduction to Plasma Theory*, Krieger, Malabar, FL, 1992.

[7] Gombosi, T. I., *Physics of the Space Environment*, Cambridge Univ. Press, Cambridge, England, U.K., 1998.

[8] Romanelli, C. C., Natarajan, A., Schaub, H., Parker, G. G., and King, L. B., "Coulomb Spacecraft Voltage Study Due to Differential Orbital Perturbations," *AAS Space Flight Mechanics Meeting*, American Astronautical Society Paper No. 06-123, 2006.

[9] Parker, G. G., Passerello, C. E., and Schaub, H., "Static Formation Control Using Interspacecraft Coulomb Forces," *2nd International Symposium on Formation Flying*, NASA Goddard Space Flight Center Paper 200600485142004.

[10] Hussein, I. I., and Schaub, H., "Invariant Shape Solutions of the Spinning Three Craft Coulomb Tether Problem," *AAS Space Flight Mechanics Meeting*, American Astronautical Society Paper No. 06-228, 2006.

[11] Parker, G., King, L., and Schaub, H., "Steered Spacecraft Deployment Using Interspacecraft Coulomb Forces," *American Control Conference*, Inst. of Electrical and Electronics Engineers, New York, 2006, p. 6.

[12] Natarajan, A., Schaub, H., and Parker, G. G., "Reconfiguration of a 2-Craft Coulomb Tether," *AAS Space Flight Mechanics Meeting*, American Astronautical Society Paper No. 06-229, 2006.

[13] Natarajan, A., and Schaub, H., "Linear Dynamics and Stability Analysis of a Coulomb Tether Formation," *Journal of Guidance, Control, and Dynamics*, Vol. 29, No. 4, July–Aug. 2006, pp. 831–839.

[14] Schaub, H., Parker, G. G., and King, L. B., "Challenges and Prospect of Coulomb Formations," *Journal of the Astronautical Sciences*, Vol. 52, Nos. 1–2, Jan.–June 2004, pp. 169–193.